

# Effect of natural oxide film on the deuterium permeation behavior of 430 stainless steel



Hongtao Huang\*, Jianpin Zheng, Shuo Ding, Weijun Wang, Huaifeng Zhang

China Institute of Atomic Energy, Beijing, 102413, China

## ARTICLE INFO

### Keywords:

Deuterium permeation  
Oxide film  
316L stainless steel  
430 stainless steel

## ABSTRACT

The deuterium permeation behavior of palladium-coated 316L stainless steel and 430 stainless steel was studied by the gas permeability testing device in this study. The results show that the deuterium permeability of the palladium-coated 316L stainless steel tested at 350 °C~650 °C was very close to the Forcey's results. This way, the conformity to some other reported results has been verified for the gas permeability testing device. The deuterium permeability for the oxidized 430 stainless steel was compared with that for the palladium-coated 430 stainless steel at temperature range of 350 °C–600 °C. The deuterium permeability for the oxidized 430 stainless steel was reduced by one order of magnitude compared with that for the palladium-coated 430 stainless steel. However, the activation energy of deuterium permeation as gas form for the oxidized 430 stainless steel was almost the same as that for unoxidized 430 stainless steel.

## 1. Introduction

Zirconium hydride is used as the reactor moderator in the thermionic space nuclear power and it easily decomposes hydrogen in the operating environment. The released hydrogen penetrates into the core through the relevant structural components, affecting the physical parameters of the reactor [1]. Compared with 316L austenitic stainless steel, 430 ferritic stainless steel has the advantages of good thermal conductivity, low thermal expansion coefficient and low sensitivity to stress corrosion cracking. It is selected as one of the alternative reactor core materials for structural components of the thermionic space nuclear power. Therefore, investigating the hydrogen permeation behavior of 430 ferritic stainless steel has important engineering application value for the development of thermionic space nuclear power. A lot of research has been carried out on the preparation and properties evaluation of hydrogen isotope permeation barrier coatings for the fusion reactor. However, 316L stainless steel or low-activity ferritic/martensitic steel was used as the substrate material in most of these studies [2–15]. There are few reports on the hydrogen isotope permeation behavior of 430 ferritic stainless steel. In the present study, the deuterium permeability of palladium-plated 316L stainless steel was first tested and compared with the reported values to verify the conformity to other reported results for the gas permeability testing device. Then the deuterium permeation behavior of the palladium-plated 430 stainless steel as well as that with natural oxide film was investigated.

## 2. Experimental method

### 2.1. Sample preparation

The 316L and 430 stainless steel used in this work are ordinary commercial stainless steel. The chemical composition of these experimental stainless steel materials are given in Table 1. Disk-type sample (32 mm diameter, 0.5 mm thickness) was used in deuterium permeation test. The disk-type samples were mechanically polished and then a palladium-plated film was formed on both sides of this sample by a CVD process, and the palladium film thickness was about 1 μm as shown in Fig. 1. The samples were connected into the gas circuit by laser welding. The thickness of the oxide film on the surface of the 430 stainless steel was evaluated by X-ray Photoelectron Spectroscopy (ULVAC-PHI QUANTERA-II SXM). The Au + sputter technique was used for the evaluation of the depth profiles of the atomic concentration.

### 2.2. Apparatus and procedure

An experimental apparatus was set up in our group to carry out the gas phase deuterium permeation test according to Fig. 2. The apparatus was divided into two parts by the samples, the high-pressure part and low-pressure part. The two parts of the apparatus were separately evacuated to less than  $4 \times 10^{-6}$  Pa. In each vacuum system, a dry

\* Corresponding author.

E-mail address: [huanghongtao401@163.com](mailto:huanghongtao401@163.com) (H. Huang).

**Table 1**  
Chemical composition of the experimental stainless steel materials (wt.%).

	C	Si	Mn	P	S	Cr	Ni	Mo	Fe
316L	0.019	0.27	0.98	0.04	0.006	16.22	10.08	2.03	Bal.
430	0.039	0.26	0.29	0.025	0.002	16.12	–	–	Bal.

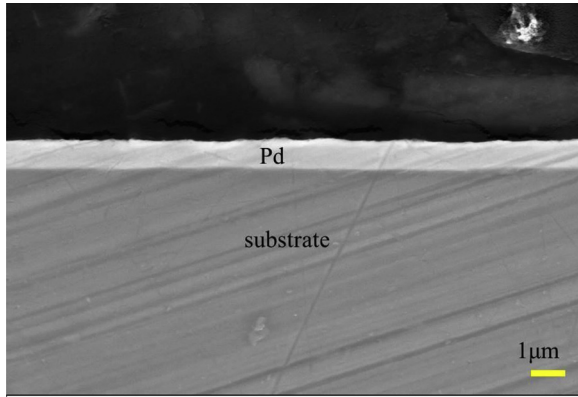


**Fig. 1.** SEM of the palladium-plated film on the stainless steel sample.

pump and a molecular pump (Pfeiffer vacuum Hipace80) were used. High purity (99.9999 %) deuterium was introduced into the high-pressure part (called upstream) at different pressures. The pressure of the upstream was measured by two vacuum gauges: a pirani gauge (Pfeiffer vacuum TPR270) and a capacitance gauge (Pfeiffer vacuum CMR371). The upstream gas inlet was equipped with a regulator tank to maintain the pressure stability during the deuterium permeation test. In the low-pressure part (called downstream), a detection chamber was designed which was a spherical stainless steel cavity with a diameter of about 200 mm and the inner surface was polished and degassed. A cold-cathode/pirani vacuum gauge (Pfeiffer vacuum PBR260) was installed at the detection chamber to detect the chamber vacuum. The partial pressure of deuterium permeating through the sample to the low-pressure part (called downstream) was measured by the quadrupole mass spectrometer (QMS, Pfeiffer vacuum QMG220M1). The detection chamber was also fitted with a standard helium leak which was used to calibrate the quadrupole mass spectrometry signals. A known helium gas flow-rate from the standard helium leak was supplied into the measuring chamber and the corresponding ion current was measured by the QMS, thus a calibration factor was obtained. This calibration factor was then used to convert any ion current measured by the QMS to deuterium permeation rates. The deuterium permeation test temperature range was 350 °C~650 °C and the deuterium pressures of the upstream were 40 kPa, 60 kPa, 80 kPa, 100 kPa in the deuterium permeation test in this work. The permeation rates were determined by the dynamic monitoring method, measuring the pressure increase in the continuously evacuated detection chamber (i.e. pumped down by a vacuum system at a constant pumping speed).

### 2.3. Simple principle

The permeation of gaseous hydrogen through materials is a complicated physicochemical process, including adsorption and dissociation of molecular hydrogen on the materials surface, solution and diffusion of the atomic hydrogen, recombination of the atomic hydrogen and desorption of the molecular hydrogen on the materials surface. The steady state permeation flux of hydrogen through materials is typically represented by the following equation [16]:

$$J_{\infty} = \frac{D \cdot S \cdot P^n}{d} \quad (1)$$

where  $J_{\infty}$  is the rate of gas permeation/unit area of the material at steady-state;  $D$  is the hydrogen diffusivity of the material– and  $S$  the hydrogen solubility for the material.  $P$  is the driving pressure,  $n$  is the pressure exponent, and  $d$  is the sample thickness. The pressure exponent  $n$  is evaluated on the basis of the pressure dependence of hydrogen permeation. A half power ( $n = 0.5$ ) dependence implies that the rate limiting process for permeation is hydrogen atom diffusion through materials, while  $n = 1$  holds for the case of surface reaction as the rate limiting process.

For the case of steady-state permeation through a single layer barrier, where the rate limiting process is diffusion through the material rather than surface reactions, the permeation rate is given by the expression [3]:

$$J_{\infty} = \frac{DS}{d}(p_h^{1/2} - p_l^{1/2}) \quad (2)$$

where  $P_h$  and  $P_l$  are the gas pressure on the high and low pressure sides respectively. The product  $DS$  is defined as the permeation coefficient or permeability  $\Phi$  of the material [3]:

$$\phi = DS \quad (3)$$

In the particular case where  $P_l$  is negligible Eq. (2) is simplified as follows:

$$\phi = \frac{J_{\infty} d}{p_h^{1/2}} \quad (4)$$

The hydrogen diffusivity  $D$  can be calculated by the time lag method [3]:

$$D = \frac{d^2}{6t_d} \quad (5)$$

where  $t_d$  is the lag time, that is the time when the transient permeation rate  $J_t = 0.617 J_{\infty}$  [17]. The hydrogen solubility  $S$  is readily calculated from the known  $\Phi$  and  $D$  according to Eq. (3).  $D$ ,  $S$  and  $\Phi$  are found to vary in the Arrhenius manner with temperature, at least at low hydrogen concentrations.

## 3. Results and discussion

### 3.1. Apparatus verification of conformity to other reported results

The palladium film prevents the sample from oxidizing during the deuterium permeation test at high temperatures. In addition, the palladium film does not affect the deuterium diffusivity in the stainless steel substrate, which is indeed independent of the surface condition. The palladium film formed on the stainless steel surface makes the kinetic surface processes faster, and this favors the closeness to diffusion limited regime and the deuterium permeability of the sample before and after palladium plating almost does not change. The deuterium permeability of palladium-plated 316L stainless steel has been tested by many researchers. Therefore, the deuterium permeability of palladium-plated 316L stainless steel was first tested and compared with the reported values to verify the conformity to other reported results for the gas permeability testing device in this work. Fig. 3 shows the deuterium permeation rate curves of palladium-plated 316L stainless steel tested at different temperatures in this work. It can be seen from the figure that the higher the test temperature, the larger the steady state permeation rate. The permeation rate above 450 °C increased first with time, then gradually decreased and tended to be stable, and formed a peak in the initial stage of permeation. This phenomenon may be related to the defect trapping effect of the hydrogen isotope. The first incoming hydrogen isotope was trapped by the microscopic defects in the material and formed a hydrogen isotope cluster, which blocked the subsequent hydrogen isotope diffusion, resulting in a decrease in permeation rate [17]. Since the defect trapping was a thermal activation process, this phenomenon only occurred above a certain temperature.

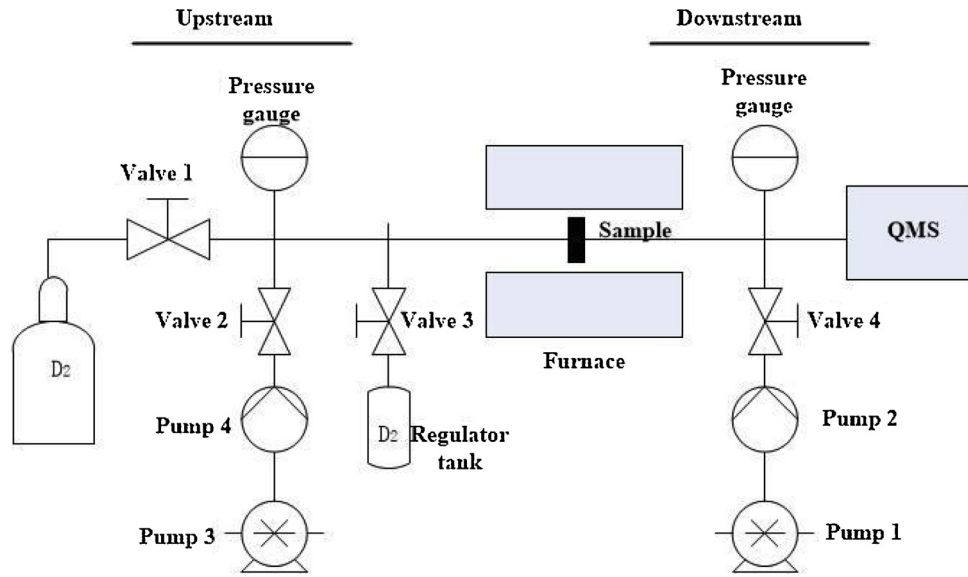


Fig. 2. Schematic view of the hydrogen permeation apparatus.

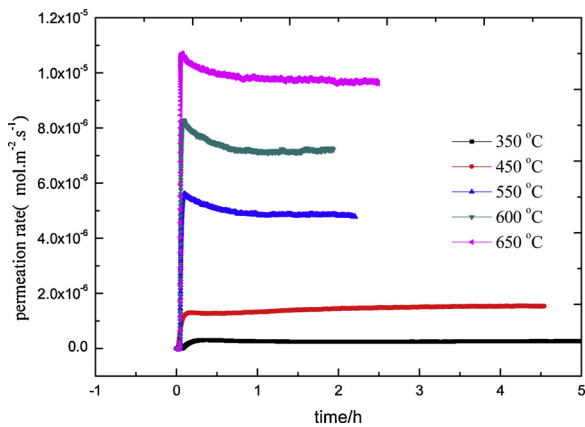


Fig. 3. Deuterium permeation rate curves of palladium-plated 316L stainless steel at deuterium pressure of 100 kPa at different temperatures.

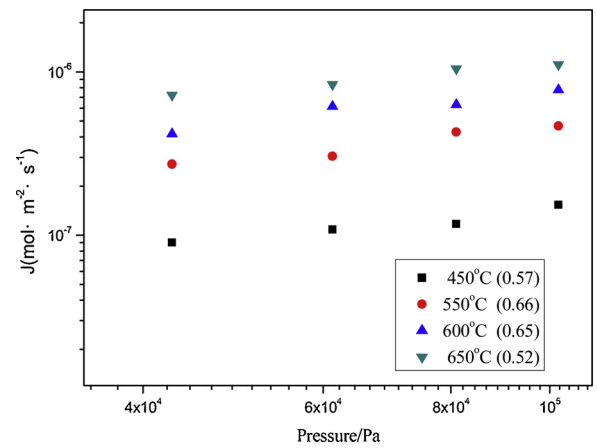


Fig. 4. Deuterium permeation rate of the palladium-plated 316L stainless steel as a function of driving deuterium pressure at different temperatures. Numbers in the parenthesis are the pressure exponents  $n$ .

However, the permeation rate below 450 °C increased with time monotonically until it reached a steady state. This was different from the shape of the curves above 450 °C. This phenomenon indicates that the diffusion coefficient changes little during the permeation process.

Fig. 4 shows the deuterium permeation rate of the palladium-plated 316L stainless steel as a function of driving deuterium pressure at different temperatures. The pressure exponents  $n$  of deuterium permeation were between 0.52 and 0.66. This indicated that the permeation regime appears to be close to diffusion limited (described with  $n = 0.5$ ), i.e. permeability is governed mainly by hydrogen transport through the bulk, whereas surface effects like adsorption and/or recombination can be neglected.

It was proposed that the surface influence of hydrogen permeation in materials was less pronounced with high driving pressures [15]. Therefore, the permeability of the palladium-plated 316L stainless steel and the 430 stainless steel was calculated at deuterium pressure of 100 kPa in this work. Fig. 5 shows the permeability of palladium-plated 316L stainless steel in this work as well as the reported values in the literatures. It can be seen that the permeability of the palladium-plated 316L stainless steel in this work is very close to the Forcey's results in the temperature range of 350 °C ~ 650 °C. The reason for this may be that the defects in the 316 stainless steel materials in this work was almost the same as that used in Forcey's work. This also indirectly verified the conformity to other reported results for the gas phase

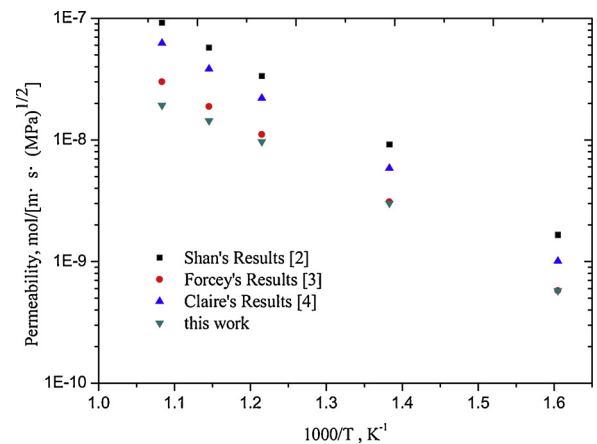


Fig. 5. Comparison of deuterium permeabilities of 316L stainless steel at different temperatures.

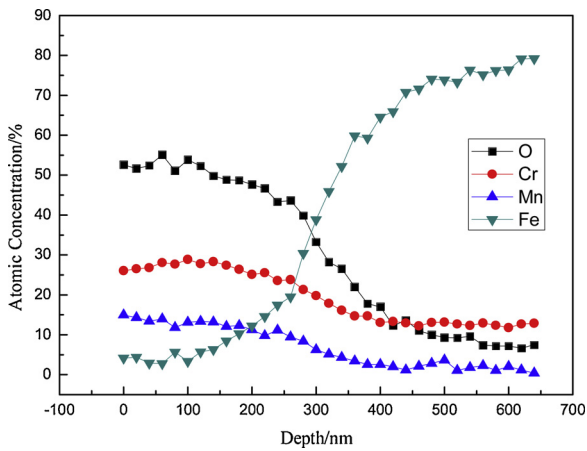


Fig. 6. XPS depth profiles of constituent atomic concentration for the 430 stainless steel with natural oxide film.

deuterium permeation test device in this work.

### 3.2. Oxide film on 430 stainless steel surface

Fig. 6 shows the depth profiles of constituent atomic concentration for the oxidized 430 stainless steel observed by XPS. It can be found that an oxide film was formed on the surface, which is about 200~250 nm thick. In the oxide layer, both the profiles of chromium and manganese have a concentration gradient and their concentrations were increased slowly toward the surface.

### 3.3. Permeation behavior of the 430 stainless steel with natural oxide film

Fig. 7 shows the deuterium permeation rate curves of the 430 stainless steel with natural oxide film tested at different temperatures in this work. The permeation rate above 350 °C increased first with time, then gradually decreased and tended to be stable, and formed a peak in the initial stage of permeation. However, the permeation rate at 350 °C increased with time monotonically until it reached a steady state. This indicates that the defect trapping effect of the hydrogen isotope was easier to occur than that of palladium-plated 316L stainless steel. This may be due to the formation of the oxide film on the surface of the 430 stainless steel and resulted in an increase in microscopic defects in the material.

For the evaluation of the deuterium permeation regime of the 430 stainless steel with natural oxide film, the deuterium pressure dependence of the permeation rate has been investigated. Fig. 8 shows the deuterium permeation rate of the 430 stainless steel with natural oxide

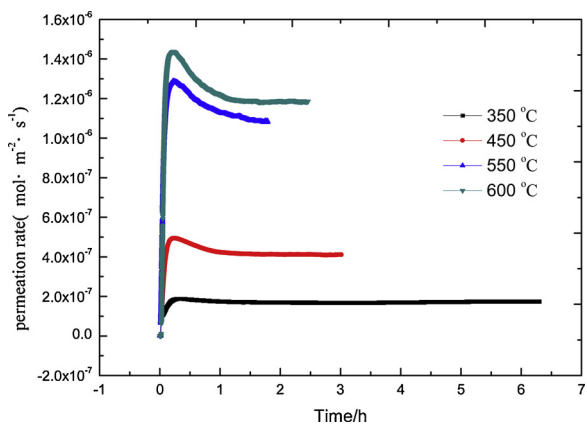


Fig. 7. Deuterium permeation rate curves of the 430 stainless steel with natural oxide film at deuterium pressure of 100 kPa at different temperatures.

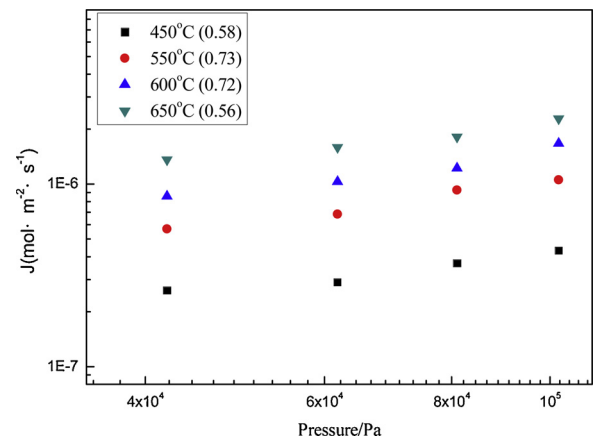


Fig. 8. Deuterium permeation rate of the 430 stainless steel with natural oxide film as a function of driving deuterium pressure at different temperatures. Numbers in the parenthesis are the pressure exponents  $n$ .

film as a function of driving deuterium pressure at different temperatures. The pressure exponents  $n$  of deuterium permeation showed 0.56~0.73. This indicated that the permeation regime appears to be close to diffusion limited (described with  $n = 0.5$ ). It is reported that the pressure exponents  $n$  between 0.5 and 1.0 were often being observed due to surface effects although the permeation was diffusion limited [3].

Fig. 9 shows the permeability of the palladium-plated 430 stainless steel as well as that with natural oxide film in this work. The deuterium permeability of the 430 stainless steel with natural oxide film was reduced by an order of magnitude and was 1/15~1/25 times as high as that for the palladium-coated one. This indicates that the natural oxide film would play as a permeation barrier and the permeation rate of deuterium as gas form was refrained. Oya et al. studied the effect of surface oxide layer on the hydrogen isotope permeation for 316 stainless steel and found that the deuterium permeability for the oxidized 316 stainless steel was reduced 1/10~1/20 times as high as that for unoxidized one [6]. Shestakov et al. investigated the permeation of deuterium through martensitic steel F82H and also found that the deuterium permeability for the oxidized sample was reduced 1/10~1/20 times as high as that for unoxidized one [7].

The deuterium permeability for the 316L and 430 stainless steel used in this work was calculated and shown as follows:

$$\text{Palladium-plated 316L: } \phi = 3.49 \times 10^{-5} \exp(-56700/RT) \quad (6)$$

$$\text{Palladium-plated 430: } \phi = 4.96 \times 10^{-6} \exp(-34500/RT) \quad (7)$$

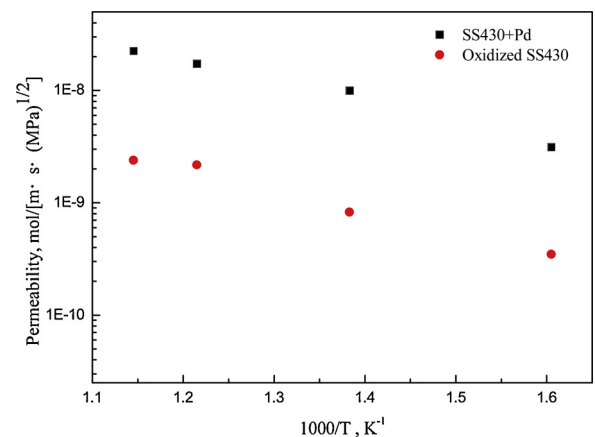


Fig. 9. Deuterium permeabilities of the 430 stainless steel as a function of temperature.

430 with natural oxide film:  $\phi = 3.96 \times 10^{-7} \exp(-36600/RT)$  (8)

Where  $\Phi$  is in  $\text{mol m}^{-1} \text{s}^{-1} \cdot \text{Mpa}^{-1/2}$ ,  $R = 8.314 \text{ J} \cdot \text{K}^{-1} \text{ mol}^{-1}$  and  $T$  is the temperature in K. The activation energy of the 316L stainless steel was about 56.7 kJ/mol. The activation energy of the 430 stainless steel was about 34.5 kJ/mol. This indicated that the deuterium permeation in the 430 stainless steel was easier than deuterium permeation in the 316L stainless steel. Moreover, the activation energy of 430 stainless steel with natural oxide film was about 36.6 kJ/mol, indicating that the activation energy of deuterium permeation as gas form was almost the same even if the oxide layer was formed on the surface or not.

#### 4. Conclusions

An experimental apparatus was set up in our group to carry out the gas phase deuterium permeation test. The deuterium permeation behavior of palladium-coated 316L stainless steel and the 430 stainless steel was investigated by this apparatus. The deuterium permeability of the palladium-coated 316L stainless steel tested at 350 °C~650 °C was very close to the Forcey's results. This indirectly verified the conformity to other reported results for the gas phase deuterium permeability testing device. The pressure exponents  $n$  of deuterium permeation of the palladium-coated 316L sample were between 0.52 and 0.66. The permeability of deuterium for the 430 stainless steel with natural oxide film was compared with that for the palladium-coated 430 stainless steel at temperature range of 350 °C~600 °C. The oxide film was about 200~250 nm thick. For this 430 stainless steel sample with natural oxide film, the pressure exponents  $n$  of deuterium permeation showed 0.56~0.73. The deuterium permeability for the 430 stainless steel with natural oxide film was reduced by an order of magnitude and was 1/15~1/25 times as high as that for the palladium-coated 430 stainless steel. However, the activation energy of the 430 stainless steel was almost the same even if the oxide layer was formed on the surface or not.

#### Declaration of Competing Interest

None.

#### Acknowledgements

The authors would like to thank Professor Hu Yong, Zhan Qin, and

Yuan Xiaoming for their help and advice in experiments and data processing, and Dr. Xiong Liangyin for the provision of palladium-plated 316L stainless steel samples. This work was supported by the Young Scientists Fund of the National Natural Science Foundation of China (grant number: 51601224).

#### References

- [1] Z.T. Su, J.C. Yang, G.T. Ke, Space Nuclear Power, Shanghai Jiao Tong University Press, Shanghai, 2016.
- [2] C.Q. Shan, Y.X. Lv, Tritium and Materials for Protection of Tritium Permeation, Atomic Energy Press, Beijing, 2002.
- [3] K.S. Forcey, D.K. Ross, J.C.B. Simpson, Hydrogen transport and solubility in 316L and 1.4914 steels for fusion reactor applications, *J. Nucl. Mater.* 160 (1988) 117.
- [4] A.D.L.E. Claire, Permeation of hydrogen isotopes in structural alloys, *J. Nucl. Mater.* 122 (1984) 1558.
- [5] K. Zhang, Y. Hatano, Sealing of pores in sol-gel-derived tritium permeation barrier coating by electrochemical technique, *J. Nucl. Mater.* 417 (2011) 1229.
- [6] Y. Oya, M. Kobayashi, J.Y. Osuo, et al., Effect of surface oxide layer on deuterium permeation behaviors through a type 316 stainless steel, *Fusion Eng. Des.* 87 (2012) 580.
- [7] V. Shestakov, A. Pisarev, V. Sobolev, et al., Gas driven deuterium permeation through F82H martensitic steel, *J. Nucl. Mater.* 307 (2002) 1494.
- [8] H.G. Yang, Q. Zhan, W.W. Zhao, et al., Study of an iron-aluminide and alumina tritium barrier coating, *J. Nucl. Mater.* 417 (2011) 1237.
- [9] G.K. Zhang, C.A. Chen, D.L. Luo, et al., An advance process of aluminum rich coating as tritium permeation barrier on 321 steel workpiece, *Fusion Eng. Des.* 87 (2012) 1370.
- [10] F.L. Yang, X. Xiang, G.D. Lu, et al., Tritium permeation characterization of  $\text{Al}_2\text{O}_3/\text{FeAl}$  coatings as tritium permeation barriers on 321 type stainless steel containers, *J. Nucl. Mater.* 478 (2016) 144.
- [11] L. Wang, J.J. Yang, Y.J. Feng, et al., Preparation and characterization of  $\text{Al}_2\text{O}_3$  coating by MOD method on CLF-1 RAFM steel, *J. Nucl. Mater.* 487 (2011) 280.
- [12] S.J. Feng, Y. Wang, C. Zhang, et al., Preparation of  $\text{Al}_2\text{O}_3/\text{Cr}_2\text{O}_3$  tritium permeation barrier with combination of pack cementation and sol-gel methods, *Fusion Eng. Des.* 131 (2018) 1.
- [13] Z.Y. Yao, A. Suzuki, D. Levchuk, Hydrogen permeation through steel coated with erbium oxide by sol-gel method, *J. Nucl. Mater.* 386 (2009) 700.
- [14] G.W. Hollenberg, E.P. Simonen, G. Kalinin, et al., Tritium-hydrogen barrier development, *Fusion Eng. Des.* 28 (1995) 190.
- [15] D. Levchuk, F. Koch, H. Maier, et al., Deuterium permeation through Eurofer and  $\alpha$ -alumina coated Eurofer, *J. Nucl. Mater.* 328 (2004) 103.
- [16] D. He, S. Li, X.P. Liu, et al., Preparation of  $\text{Cr}_2\text{O}_3$  film by MOCVD as hydrogen permeation barrier, *Fusion Eng. Des.* 89 (2014) 35.
- [17] S. Liu, H. Zheng, Q.H. Gui, et al., Measurements of hydrogen diffusion coefficient for tube samples at medium and high temperatures, *Acta Metall. Sin.* 40 (2004) 393.